

Supplementary Materials

An EGFR signature predicts cell line and patient sensitivity to multiple tyrosine kinase inhibitors

Chao Cheng^{1,2,3*}, Yanding Zhao⁴, Evelien Schaafsma⁴, Yi-Lan Weng⁵, Christopher Amos^{1,2,3}

Table of contents

Supplementary Figures

Suppl. Figure 1. Correlation between EGFR scores and EGFR mRNA abundance.

Suppl. Figure 2. Correlation between EGFR scores and the average methylation level of CpG sites at the EGFR gene body region.

Suppl. Figure 3. Boxplot depicting EGFR score differences between Erlotinib sensitive and resistant lung cancer cell lines.

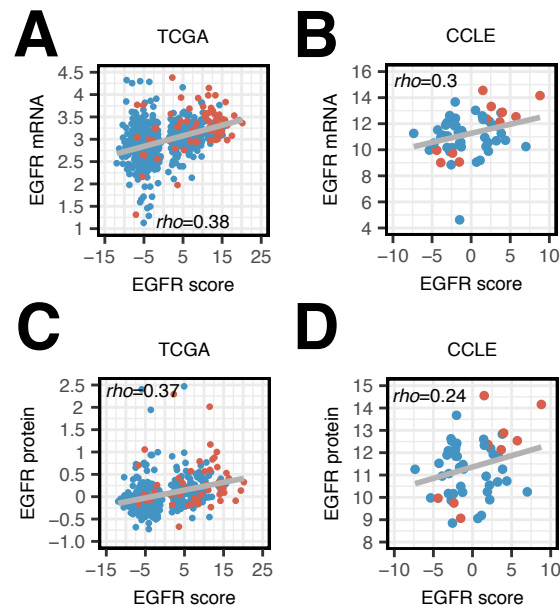
Supplementary Tables

Suppl. Table 1: Overview of utilized datasets.

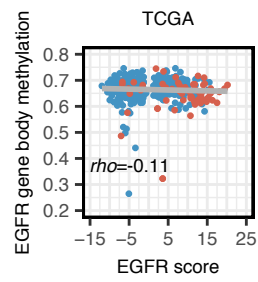
Suppl. Table 2: Weights of genes in the EGFR signature.

Suppl. Table 3: Pathway enrichment analysis.

Suppl. Table 4: Identifiers of samples used in this study.



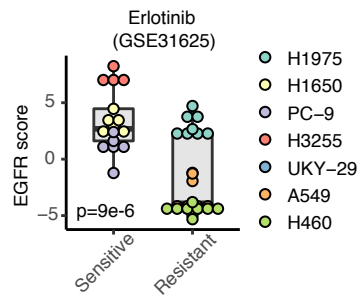
Suppl. Figure 1. A-B, Correlation between our EGFR score and EGFR mRNA abundance in TCGA lung adenocarcinoma tumor samples **(A)** and CCLE lung cancer cell lines **(B)**. **C-D,** Correlation between EGFR scores and EGFR protein abundance in TCGA lung adenocarcinoma tumor samples **(C)** and CCLE lung cancer cell lines **(D)**. In all scatterplots, ρ indicates Spearman correlation coefficient.



Suppl. Figure 2. Correlation between EGFR scores and the average methylation level of CpG sites at the EGFR gene body region. ρ indicates Spearman correlation coefficient.

40

41



42

43

44

45

46

Suppl. Figure 3. Boxplot depicting EGFR score differences between Erlotinib sensitive and resistant lung cancer cell lines. The p-value was calculated by the one-tailed Wilcoxon rank-sum test.

52 **Suppl. Table 3:** Pathway enrichment analysis. For each enrichment term of genes
 53 in EGFR signature, its pathway term, geneset size, number of overlapped genes,
 54 enrichment ratio, P-value and FDR are provided.

Term	Geneset		Enrichment		
	t Size	Count	t ratio	PValue	FDR
KEGG_ASTHMA	28	11	9.67	5.30E-09	5.35E-06
KEGG_INTESTINAL_IMMUNE_NETWORK_FOR_IGA_PRODUCTION	46	13	6.96	2.19E-08	1.11E-05
KEGG_ALLOGRAFT_REJECTION	35	11	7.74	7.94E-08	2.67E-05
KEGG_GRAFT_VERSUS_HOST_DISEASE	37	11	7.32	1.51E-07	3.81E-05
KEGG_TYPE_I_DIABETES_MELLITUS	41	11	6.60	4.81E-07	9.70E-05
KEGG_LEISHMANIA_INFECTION	70	14	4.92	6.95E-07	1.17E-04
KEGG_VIRAL_MYOCARDITIS	68	13	4.71	2.96E-06	4.26E-04
KEGG_AUTOIMMUNE_THYROID_DISEASE	50	11	5.42	4.07E-06	5.13E-04
KEGG_CELL_ADHESION_MOLECULES_CAMS	131	18	3.38	5.98E-06	6.04E-04
KEGG_ANTIGEN_PROCESSING_AND_PRESENTATION	81	13	3.95	2.18E-05	1.83E-03
REACTOME_TRANSLOCATION_OF_ZAP_70_TO_IMMUNOLOGICAL_SYNAPSE	13	6	11.36	5.93E-06	6.04E-04
REACTOME_PHOSPHORYLATION_OF_CD3_AND_TCR_ZETA_CHAINS	15	6	9.85	1.61E-05	1.48E-03
REACTOME_PD1_SIGNALING	17	6	8.69	3.72E-05	2.88E-03
REACTOME_GENERATION_OF_SECOND_MESSENGER_MOLECULES	26	7	6.63	5.95E-05	4.29E-03
REACTOME_MHC_CLASS_II_ANTIGEN_PRESENTATION	90	12	3.28	2.78E-04	1.87E-02

55